ORIGINAL RESEARCH

Novel Cold Cure Acrylic Denture Base with Recycled Zirconia Nano-Fillers That Were Functionalized by HEMA Agent Incorporation: Using the Sprinkle Approach

Hala B Elzahar[1,2], Mohamed S El-Okaily[3], Mohamed H Khedr[2], Mohamed Amgad Kaddah[1], Ahmed AG El-Shahawy[2]

[1]Faculty of Dentistry-Cairo University, Department of Orthodontics, Cairo, Egypt; [2]Materials Science and Nanotechnology Department, Faculty of Postgraduate Studies for Advanced Sciences (PSAS), Beni-Suef University, Beni-Suef, Egypt; [3]Nanomedicine & Tissue Engineering Laboratory, Medical Research Center of Excellence (MRCE), Refractories, Ceramics & Building Materials Department (Biomaterials Group), National Research Centre, Cairo, Egypt

Correspondence: Ahmed AG El-Shahawy, Tel +20 1226798209, Email Ahmed.elshahawy@psas.bsu.edu.eg

Background: Though acrylic resins possess many useful properties, denture fracture is nevertheless a familiar issue.

Objective: This study aimed to determine the effect of low-percent recycled Zirconia nanoparticles as filler on the transverse strength, impact strength, surface hardness, water sorption, and solubility of resin using the sprinkle cold-curing technique.

Materials and Methods: Various formulae were prepared and mixed with PMMA (polymer) powder containing varying percentages (0.01%, 0.1%, 0.3%, and 0.5%) of recycled ZrO2NPs to mono-methyl methacrylate (MMA monomer). A 2-hydroxyethyl-methacrylate (HEMA) agent was used to functionalize recycled zirconia (ZrO_2) nano-fillers. X-ray diffraction, field emission scanning electron microscopy, high-resolution transmission electron microscopy, energy-dispersive X-ray spectroscopy, and dynamic light scattering were used to characterize the samples. For mechanical tests, standard metallic moulds (according to American Dental Association specification no. 27) were machined for 60 specimens' preparation, 12 for each percent (zero, 0.01%, 0.1%, 0.3%, and 0.5%). A one-way ANOVA test was used to compare the five groups for parametric data, while the Kruskal–Wallis test was employed for nonparametric data. The P 0.05 value was accepted as the significance level. All formulae were tested for cytotoxicity at 24 and 48 hours on WI38 normal lung cell lines.

Results: The XRD analysis demonstrated the tetragonal crystallographic structure of the recycled zirconia nanoparticles. Incorporating a low percentage of recycled ZrO_2 nanoparticles (0.01%, 0.1%, 0.3%, and 0.5%) improved the tested properties of PMMA to different degrees in a significant and non-significant pattern, while the optimal tested percent was 0.3%.

Conclusion: The 0.3% percentage of recycled zirconia nanoparticles maintained and improved the physical and mechanical properties of acrylic resin. Recycled ZrO_2/PMMA nanocomposite is a synergistic candidate due to its economic return and clinical application safety.

Keywords: acrostone, cold cure, novel, recycled zirconia, sprinkle

Background

In dentistry, acrylic resins (ARs) are prevalent as a denture base material. These resins are convenient substances and are employed in the oral environment owing to their adequate physiological and chemical characteristics, ease of handling, positive aesthetic, and low cost.[1] Acrylic resin comprises powder and liquid components. The powder includes spheres of polymethyl methacrylate (PMMA) and a small amount of benzoyl peroxide as an initiator, while the liquid is methacrylate with a trace of hydroquinone as an inhibitor. Glycol di-methacrylate is a cross-linking agent to deform plasticizers such as di-butyl phthalate.[2]

Polymerization is the common process of synthesis of acrylic resins. Two methods to initiate the polymerization of PMMA are heat-cured and cold-cured, which are called self-cured or auto polymerization.[3] Heat-cured is used for removable full dentures or removable partial dentures, while cold-cured is used for denture repair, relining, and orthodontic removable appliances involved in thumb deterrent, tipping teeth, block movements, overbite reduction, space maintenance, and retention.[4] Furthermore, cold-cured acrylic resin is one of the most commonly used materials in dentistry for maxillofacial prostheses, with its use in crowns and bridgework providing temporary coverage of prepared teeth.[5]

Cold-cured acrylic resin is the same as the heat-cured acrylic resin denture base material. However, the fundamental difference is the step of polymerization initiation at room temperature.[6] Regarding this step, in all PMMA polymers used in dentistry, there is a small percentage of a peroxide catalyst. This peroxide is broken into free radicals by heat, which catalyses the polymerization reaction. However, heat affects the chemical reaction maturity of acrylic resin and will alter the properties of the cured resin.[7] Furthermore, heat-curing takes a long time and induces denture distortion.[8] While in cold-cured acrylic, a tertiary amine is added to the liquid monomer to allow the peroxide to be liberated as a catalyst without heat.[9] The limitation of the cold-cured is the low degree of polymerization, and the unreacted or residual monomer is greater than in the heat-cured. For this reason, one of the critical faults of the cold-cured acrylic resin is its lack of mechanical hardness and strength. This is our key point in the presented research.

Indeed, for several years, the cold-curing acrylic resin has been subjected to critical analysis.[10] Its future is still somewhat controversial. Many attempts have been made to improve the mechanical properties of cold-cured PMMA, including its chemical modification, but they have only delivered a limited reinforcement effect.[11] The search of literature reveals that the addition of varying amounts of metal fillers such as powdered silver, copper, and aluminium into PMMA at various concentrations not only gives it an advantage of increased strength and improved thermal conductivity, but also reduces the polymerization shrinkage, decreases the warpage, makes the material radiopaque, and inhibits the growth of bacteria over the denture surface.[12] However, the major disadvantage of adding metal fillers is its compromised esthetics.

Nanotechnology is used in the dental field as nano dentistry. Choosing the nanoparticles NPs for use in the field of nano dentistry, its chemical, physical, and biological aspects are taken into account.[13] Benjamin et al[14] worked on the mechanical properties of Al_2O_3/PMMA nanocomposites. Al-Kawaz et al[15] investigated the mechanical properties of acrylic-based nanocomposite coatings reinforced with PMMA grafted-multi-wall carbon nanotubes (MWCNT). Sushil et al[16] studied the effect of TiO_2 NPs on the mechanical properties of epoxy-resin systems. Navidfar et al[17] studied the influence of processing conditions and carbon nanotubes on the mechanical properties of injection moulded MWCNT/PMMA nanocomposites. Different percentages of TiO_2 NPs as reinforcement to a base material, PMMA, were investigated by Md. Alamgir et al.[18]

Recently, nano-zirconia has found broad applications in energy and biomedical applications because of its unusual combination of strength, fracture toughness, ionic conductivity, and low thermal conductivity.[19] Previous research investigated the effect of reinforcing resin with 5% and 15% ZrO_2 and concluded that reinforcement of high-affected resin with zirconium powder increases its transverse strength. Another study looked at how ZrO_2 content and morphology (nanotubes/nanospheres) affected mechanical properties like impact, flexural, and hardness.[20] Further research has recommended different concentrations of zirconia filler reinforcements for the various acrylic resin systems.

Being cold-cured acrylic resin is widely used in prosthetic work because of its simple technique at room temperature, is less time-consuming, and requires less equipment. For this reason, in our study, we paid special attention to cold-cured, and the selection of nano-ZrO_2 as a filler was based on the properties of this filler, which can improve the mechanical properties of acrylic resins. Furthermore, from an economic standpoint and because there is no available data in the literature regarding the effect of recycled zirconia metal oxides with low percent on cold-cured PMMA, in this research, the reinforcement of denture base PMMA with recycled ZrO_2 NPs was studied for the first time. In this light, the key point of our study was to develop the mechanical and physicochemical properties of a cold-cure acrylic resin (Acrostone, Figure S1) made from PMMA that was doped with recycled zirconia (ZrO_2) nano-fillers. These were remaining zircon particles, waste products from zircon discs used in CAD/CAM devices used in fixed dental bridges (Figure S1). Before doping, the recycled zirconia (ZrO_2) nano-fillers were functionalized with a 2-hydroxyethyl-methacrylate (HEMA) coupling agent.

The objectives of the current study were divided into three phases. The first phase involved the preparation of recycled Zirconia nanoparticles (ZrO_2 NPs) and surface functionalization with HEMA coupling agent. Various formulae

were prepared and mixed with PMMA (polymer) powder containing varying percentages (0.01%, 0.1%, 0.3%, and 0.5%) of recycled ZrO2NPs-HEMA to mono-methyl methacrylate (MMA monomer). In the second phase, regarding the prepared formulae, several factors such as crystallinity, size, surface potential, morphology, and the dispersion of the modified zirconia were characterized using various advanced techniques. In the 3rd phase, the effect of those percentages on the cold-cured acrylic resin was evaluated from the point of hardness as a surface mechanical property, flexure strength or transverse strength, impact, and modulus of elasticity tests. Further, we studied the chemo-physical properties (water sorption-solubility) and cytotoxicity of normal cell lines in vitro. The study's hypothesis was that a low-percentage addition of recycled nano-ZrO_2 would maintain or improve the properties of the PMMA denture base materials, and that this would have an economic impact.

Materials and Methods

Materials

The used materials were recycled zirconia nanoparticles (size: 200–250 nm, cubic crystal), 2-hydroxyethyl methacrylate (HEMA) as coupling agent, Azo-bis iso-butyronitrile (AIBN), ethanol, and benzyl alcohol, Xylene, and a commercial denture material (Acrostone) acrylic resin Figure S1A. The latter is composed of a two-component system, including powder (PMMA polymer) and liquid (MMA monomer). The powder comprises a PMMA polymer and the initiator benzoyl peroxide (BPO). The liquid includes an MMA monomer with a small amount of ethylene glycol-di-methacrylate (EGDMA) that is used as a chemical activator.

Methods

Formulae Preparation

Ball Milling Technique

Again, we recycled the remaining zircon particles, waste products from zircon discs (Cermill Zolid ht+ white, German) used in CAD/CAM (computer-aided-design/computer-aided-manufacturing) devices used in fixed dental bridges, Figure S1B. The recycled ZrO_2 NP_S was prepared by mechanical attrition through the ball milling process using a planetary ball mill (Fritsh planetary Mono Mill Pulverisette6). A 250 mL Agate bowl with a matching lid and three to five 2.5 cm fused alumina grinding balls were used. The milling time was restricted by the generated heat during the grinding process. Therefore, the milling time was 20 min at a speed of 300 rpm, and the cooling time was 30 min. The milling cycle comprises milling and cooling time. The number of cycles was 9, so the total milling time was 3 hours per day, and we repeated the milling for three days.

Preparation of Recycled ZrO_2 NPS Dispersed in MMA (Liquid Monomer) with Different Percentages

The prepared recycled ZrO_2 NPS was suspended in benzyl alcohol, centrifuged in benzyl alcohol, washed with xylene with two repeated sonication cycles for 3 minutes, and centrifuged again at 1500 rpm for 3 minutes. The collected wet recycled ZrO_2 NPS comprised 45 wt% of xylene. Surface functionalization of wet recycled ZrO_2 NPS was performed by using HEMA coupling agents, in which the amount of HEMA was generally designed based on the HEMA-to-ZrO_2 molar ratio of 0.8/1.[21] Through a planned design, specific molar ratios of the wet recycled ZrO_2 NPS, HEMA, and MAA were stirred to prepare different liquid samples with recycled ZrO_2 ratios (0.01%, 0.1%, 0.3%, and 0.5%).

In-situ Polymerization of the Recycled ZrO_2 NPS- HEMA-MMA with PMMA Polymer

The acrylic resin production was done through a familiar sprinkle-on technique. In this technique, the PMMA powder polymer was sprinkled into moulds to form a thin, uniform layer. Next, we added the prepared liquid samples containing ZrO2NPs-HEMA-MMA with the mentioned percentages separately, using a syringe to soak the powder. The total moulds were preserved in a pressure container at a temperature of 41°C (2.4 bar, Figure S1) for 15 minutes.[22] The polymerization reaction was carried out at room temperature with mechanical stirring for approximately 4–5 minutes, or until the reactants reached the desired viscosity and dough stage.

Characterization

X Ray Diffraction (XRD)

Crystalline phase identification of the ZrO_2 powders was done by XRD. Using Cu K (= 1, 54) radiation, we used XRD to characterize the crystallinity of the material. The device worked with a 30 mA current, a functioning voltage of 40 kV (power of 1200 W), and a scanning speed of 2/min (step size = 0.050 and step time = 1.5s) in the 10–80 scanning range (2 Theta scale) at room temperature. The crystalline phases were determined by matching the corresponding International Center for Diffraction Data (ICDD) cards.

Morphology Study of the Prepared Specimen

The particle size of the prepared formula was determined by a high-resolution transmission electron microscope (HR-TEM) using a JEM 1400 (Japan) operated at 300 kV. A Field Emission Scanning Electron Microscope (FESEM; using a Philips-XL30 device, Netherlands) was employed to investigate the surface morphology, map images to detect the elemental spatial resolution, and perform energy dispersive X-ray EDX for elementary analysis. The microscopy samples were prepared with dispersion in deionized water at room temperature. The zeta potential was measured by the Zetasizer Nano-ZS90 (Malvern, UK).

Mechanical Properties

For mechanical tests, 60 specimens, 12 for each group (Zero, 0.01%, 0.1%, 0.3%, and 0.5%) were prepared, dried overnight at 60 °C, and stored at room temperature to remove the xylene and the residual monomers. According to the international guidelines, the specimens were packed in specific moulds for investigations with standard dimensions. All the specimens' dimensions of the mechanical properties, water sorption, solubility, and cytotoxicity will be mentioned in detail.

Impact Strength Test. The impact strength of the specimens was measured according to ASTM D 6110 using the Charpy impact tester (DIGTAL IZOD), Figure S2A. The specimens' dimensions were (75 mm in length x 10 mm in width x 10 mm). The specimens were gripped horizontally and were broken by a single swing of the pendulum of 2 J. The pendulum struck the specimen in the middle, directly opposite to the notch (blue arrow in Figure S2B). The impact strength in Joules (J) was obtained directly from the machine.[23]

Flexural Strength Test. Specimens (65 mm in length x 10 mm in width x 2.5 mm), Figure S3A were tested under static loading using the universal testing machine (AMETEK-LLOYD LRX-Plus) under 3-point loading, Figure S3B. Each specimen was placed on two parallel stainless steel rods (10 mm in diameter) located 40 mm apart. We applied a central compressive force until fracture using a cylindrical stainless steel rod with a diameter of 10 mm and a crosshead speed of 0.5 mm/min. The software attached to the testing machine was used to get the load-extension curve of the tested specimen. According to the American Society for Testing and Materials (ASTM),[24] the maximum flexural strength of each specimen was calculated from the following formula:

$$\sigma = \frac{3PL}{2bd^2}$$

Where: flexural strength (MPa), P: fracture load (N), L: distance between supporting rods (40 mm), b: specimen width (10 mm), and d: specimen thickness (2.5 mm).

Modulus of Elasticity. The test specimens for transverse strength and modulus of elasticity were made following ISO 20795–1, an international standard. Test specimens were prepared to have dimensions of 65 mm in length x 10 mm in width x 2.5 mm, Figure S3A. A three-point bending test was applied for transverse strength and modulus of elasticity, and force was applied until failure occurred with a universal testing machine (AMETEK-LLoyd LRX-Plus) at the midpoint of the specimens. The device's speed was determined using the ISO 20795–1 standard (5 mm/min). The transverse strength and modulus of elasticity are calculated using the following formula:[25]

$$E = FI3/4bh3\,d$$

(E = modulus of elasticity (MPa), F = maximum load at the moment of fracture (N), l = distance between the supports, b = specimen width, and h = specimen thickness, mm).

Hardness. Hardness was tested using the fractured specimens from impact strength testing; these specimens had dimensions of 37.5 mm in length x 10 mm in width x 10 mm in height. A disc was prepared for testing. A Digital Vickers Micro-hardness tester (Reichert, Austria, Figure S4A) was used for testing surface hardness. The specimens were polished from one surface, and a 50 gf load was applied for 5 seconds of indentation time, and VHN was obtained digitally.

Water Sorption and Solubility

Sorption and solubility were determined by the method described in Specification 12 of the American Dental Association (ADA) for base polymers for dentures. The identified sample by percentage was weighed on an analytical scale with a precision of 0.2 mg and was placed in a rack within a desiccator containing dried silica gel to conduct the sorption and solubility experiments, Figure S4B. The desiccator was placed in an oven at 37 °C ± 1.0 °C for 24 hours, and then it was removed and left to cool for one hour until it reached room temperature (23 °C ± 1 °C). The method was continued until the mass loss of each sample was less than 0.2 mg, resulting in a constant mass, *M1*, or "conditioned mass."

The volume of each sample was estimated by taking the average of three diameter measurements. An average of five thickness measurements was taken at the center and four sites equidistant from the circumference of each sample. Subsequently, the samples were immersed in bi-distilled water at 37 °C ± 1.0 °C for seven days. After that period, they were removed from the water with tweezers, weighed one minute after they had been removed from the water, with an accuracy of 0.2 mg, the weighted mass recorded as *M2*, dried with a cloth until they were free of moisture, and agitated in the air for 15 seconds. The sample was "reconditioned" in the desiccator using the process described above until it attained a consistent mass. The "reconditioned" mass was recorded as an *M3* mass.

Water Sorption Test. As mentioned, the specimens' dimensions of the water sorption and solubility are reported in Table 1.

$$\text{Water sorption } (\mu \text{g/mm}^3) = M2 - M3/V$$

Where M2 is the mass of the disc in micrograms after immersion, M3 is the reconditioned mass of the disc in micrograms, and V is the volume of the disc in cubic millimeters.

The disc's volume (in mm3):

V = πr 2 x h Where r = the radius of the disc in mm and h = the height in mm.

Solubility Test.

$$\text{Solubility } (\mu \text{g/mm3}) = M1 - M3/V$$

Where M1 is the conditioned mass of the disc in micrograms, M3 is the reconditioned mass of the disc in grams, and V is the volume of the disc in cubic millimeters. The water sorption and water solubility per unit volume were determined according to ISO standard 1567: 1999.[26] The value of the water sorption (Wsp) of each sample, expressed in micrograms per cubic millimetre (μg/mm3), was calculated.

Cytotoxicity

Specimens were moulded to form cubics with dimensions of 1 cm in length x 1 cm in width x 2 mm in height. The cytotoxic effect of the specimens was determined versus WI38 normal lung cells. The flasks of W138 cells were purchased from the Egyptian VACSERA (Figure S4C). The viability test was conducted at VACSERA, following all the approved institutional regulations. Cell viability was evaluated by the MTT assay, which is based on the ability of the mitochondrial enzyme succinate dehydrogenase to convert the yellow water-soluble tetrazolium salt (MTT) into formazan crystals in metabolically active cells. This water-insoluble, dark blue product is stored in the cytoplasm of cells and becomes soluble afterwards, generating a blue color. The colour intensity is directly proportional to the number of viable cells. The cells were first cultured in a 96-well plate (Figure S4C) with DMEM for 24 hours and then starved for 6 hours. Next, the cells were incubated for 48 hours with the prepared specimens in the cell medium. After incubation

Table I Summarize All the Data of Mechanical Properties, Water Sorption and Solubility

	Group	No. of Samples	Mean	SD	P-value	Effect Size (Eta Squared)
Micro-hardness (VHN)	Pure without ZrO_2	12	17.82[B]	0.95	0.002*	0.262
	ZrO_2 0.01%	12	19.41[A]	1.68		
	ZrO_2 0.1%	12	17.82[B]	0.95		
	ZrO_2 0.3%	12	17.99[B]	1.01		
	ZrO_2 0.5%	12	17.82[B]	0.61		
Impact strength (KJ/m^2)	Pure without ZrO_2	12	7.31[A]	1.26	< 0.001*	0.381
	ZrO_2 0.01%	12	6.92[AB]	1.38		
	ZrO_2 0.1%	12	5.6[C]	0.91		
	ZrO_2 0.3%	12	5.69[BC]	1.16		
	ZrO_2 0.5%	12	5.05[C]	0.89		
Young's modulus of bending (MPa)	Pure without ZrO_2	12	1248.3[C]	243.4	< 0.001*	0.495
	ZrO_2 0.01%	12	1419.5[B]	139.8		
	ZrO_2 0.1%	12	1475.7[B]	201.9		
	ZrO_2 0.3%	12	1698.5[A]	137.7		
	ZrO_2 0.5%	12	1706.8[A]	175.1		
Flexural strength (MPa)	Pure without ZrO_2	12	56.6[B]	9.1	< 0.001*	0.396
	ZrO_2 0.01%	12	59.9[B]	9.3		
	ZrO_2 0.1%	12	60[B]	7.8		
	ZrO_2 0.3%	12	74.8[A]	5.1		
	ZrO_2 0.5%	12	69.5[A]	11.6		
Water sorption ($\mu g/mm^3$)	Pure without ZrO_2	12	17.05[B]	2.2	< 0.001*	0.373
	ZrO_2 0.01%	12	16.79[B]	1.84		
	ZrO_2 0.1%	12	17.31[B]	0.78		
	ZrO_2 0.3%	12	17.55[B]	2.17		
	ZrO_2 0.5%	12	20.33[A]	1.28		
Solubility ($\mu g/mm^3$)	Pure without ZrO_2	12	0.491[B]	0.237	< 0.001*	0.628
	ZrO_2 0.01%	12	0.348[B]	0.229		
	ZrO_2 0.1%	12	0.741[B]	0.266		
	ZrO_2 0.3%	12	1.91[A]	1.606		
	ZrO_2 0.5%	12	1.745[A]	0.54		

Note: *Significant at $P \leq 0.05$. According to a pair-wise statistical test for comparisons among the investigated groups, the superscripts A, B, and C indicate that these groups are statistically significant.

periods of 48 hours, 200 L of MTT (Sigma, St. Louis, Mo.) was added to each well of tested cells, followed by 4 hours of incubation at 37C and 5% CO_2. The medium was then removed and the Formazan crystals were dissolved with 120 mL per well of dimethyl sulfoxide (DMSO) for 30 minutes on a plate shaker, generating a blue color. Optical density was

read at 550 nm (microplate reader, Biorad, Tokyo, Japan). A Biotek 8000 (USA) ELISA plate reader was used to measure optical densities. The Master–Plex-2010 programme was used to calculate the IC_{50} of test extracts. Data was reported for three independent experiments. The viability percentage was calculated as follows: (OD of treated cells/OD of untreated cells) X 100 = cell viability percentage.[27] The IC_{50} of test venoms was determined using the Master–Plex-2010 program.

Statistical Analysis

Data was explored for normality by checking the distribution of data and using tests of normality (Kolmogorov–Smirnov and Shapiro–Wilk tests). All the data showed a normal (parametric) distribution except for the solubility data, which showed a nonparametric distribution. The data was presented as mean and standard deviation (SD) values. For parametric data, a one-way ANOVA test was used to compare between the five groups. When the ANOVA test was significant, Tukey's test was used for pair-wise comparisons. For nonparametric data, the Kruskal–Wallis test was used to compare between the five groups. Dunn's test was used for pair-wise comparisons when the Kruskal–Wallis test was significant. The significance level was set at $P \leq 0.05$. Statistical analysis was performed with IBM SPSS Statistics for Windows, Version 23.0. IBM Corp., Armonk, New York. A two-way ANOVA test was used to compare the viability percentage between the five groups as well as to study the changes over time within each group.

Results

Qualitative Analysis of XRD

Figure 1A exhibits the XRD spectrum of the recycled zirconia NPS in powder form. The spectrum was well-matched with the International Center for Diffraction Data ICDD cards. The XRD pattern reflected a mixed crystal structure because of its diffraction peaks of the monoclinic (pdf Card No. 00-065-0687) and tetragonal phases (pdf Card No. 04-014-2971). The revealed tetragonal phase ZrO_2 (t-ZrO_2) had a crystal lattice structure and space group p24/nmc. The lattice parameters were (a) 3.5900, (b) 3.5900, and (c) 5.1600 Å, (α) 90°, (β) 90°, and (γ) 90°. The figure showed diffraction peaks at 2θ° [30°.3, 34°, 35°, 50°.3, 50°.8, 60°.8, 63°, 68°.8] with corresponding diffraction plans (011), (002), (110), (112), (200), (211), (202), and (212). The diffraction peaks were sharp and narrow and reflected the high crystallinity of the recycled zirconia NPS. The decreased width of the diffracted peaks reflected the high purity of the recycled zirconia NPS and showed an increase in the average crystallite size. It is visible that the recycled zirconia NPS was high crystalline with no other crystalline byproducts present, in agreement with Garnweitner[28] and Reyes-Acosta.[29] The strong peak centred at 30.3 (101) is observed, showing the tetragonal structure. The peak was a relative intensity of [100%], 2.94964 d-spacing [Å], crystallite size 471.934700 [Å], and ε-MicroStrain developed during synthesis was 0.312505 [%]. The high intensity of this peak reflected the purity of the recycled zirconia. The peak prior to (101) indicated a monoclinic phase. The diffraction pattern of pure PMMA, Figure 1B, showed a broad diffraction peak at $2\theta° = 22.5$, typical of an amorphous material, together with two bands of variant intensity centred at 12.7 and 33.7. The diffraction patterns of ZrO_2/PMMA 0.3% nanocomposites showed the same broadband observed in pure PMMA, indicating that neither the ZrO_2 NPs nor the preparation process changed the orientation of the PMMA chains and did not change the amorphous nature of PMMA. Observing the ZrO_2 characteristic crystalline band revealed that the zirconia was embedded in the PMMA matrix.

Morphology Study

The ZrO_2/PMMA nanocomposite samples were characterized by HR-TEM to substantiate the dispersion of ZrO_2 NPs. Figure 2 shows HR-TEM images of recycled zirconia in different phases. Figure 2A was pure ZrO_2 with varying size distributions and high agglomeration. Further milling procedures and after the first, second, and third milling processes (Figure 2B–D, respectively), the particle size decreased to an average of 50 nm, the particle distribution was homogeneous, and well-distributed, as shown in Figure 2D. The TEM micrographs show ZrO_2 nanocrystals with faced-shaped, and most of the ZrO_2 NPs are in tetragonal shapes. The results agree with the XRD. Using HR-TEM imaging, the selected area electron diffraction pattern SEADP of ZrO_2NPs was displayed in Figure 2E. The arranged concentric rings with the bright signal intensity of SEAD and HR-TEM images confirm that ZrO_2NPs have good and regular ploy crystallinity. Figure 2F presents the d-spacing, also known as lattice spacing or interplanar distance, of a crystal. The measured value was roughly 0.3 nm, with good agreement with those reported in XRD (101).
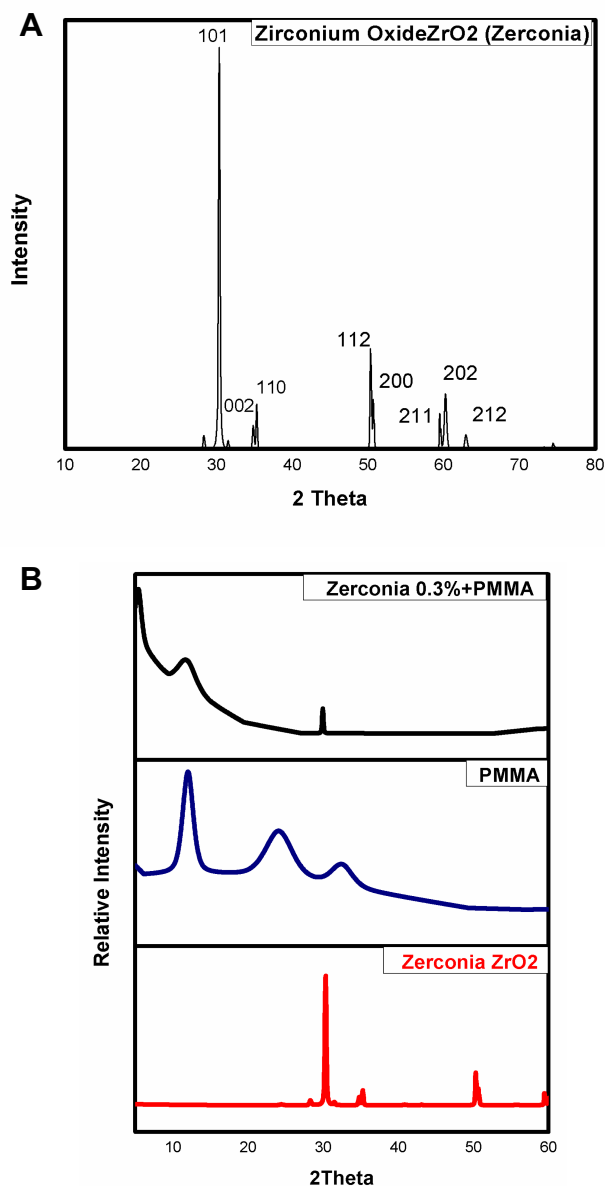
Figure 1 (**A**) exhibits the XRD spectrum of the recycled zirconia NPS in powder form, while (**B**), shows XRD of 0.3% ZrO_2, pure PMMA, and ZrO_2/PMMA 0.3% nanocomposites.

It is worth mentioning that the process for preparing the ZrO_2/PMMA nanocomposite not only homogenised the dispersion of ZrO_2 NPs in the PMMA matrix but also improved the compatibility among them. Figure 3 shows the FE-SEM images of PMMA plank (Figure 3A) and ZrO_2 (0.3%)/PMMA nanocomposite (Figure 3B). The observed bright spots in Figure 3B reflect the homogenous and uniform distribution of ZrO_2NPs in the PMMA matrix. The ZrO_2 (0.3%)/PMMA matrix seems to be rougher than the blank matrix, and the roughness increases as the weight percent of ZrO_2 increases. The surface of the blank was smooth, exhibiting brittle fracture characteristics. The recycled ZrO_2 filler NPs were inserted into and bonded to the PMMA matrix, filling the inter-polymeric chain spaces, demonstrating a robust connection and reflecting the importance of the recycled ZrO_2 addition.

Energy dispersive x-ray EDX is an interaction between X-rays and the investigated compound, providing quantitative and qualitative information about the chemical composition of that compound. Figure 3C presents the EDX spectra of the ZrO_2 (0.3%)/PMMA nanocomposite. The spectrum revealed the C and O element content with weightings of 40.4 and 59.6,
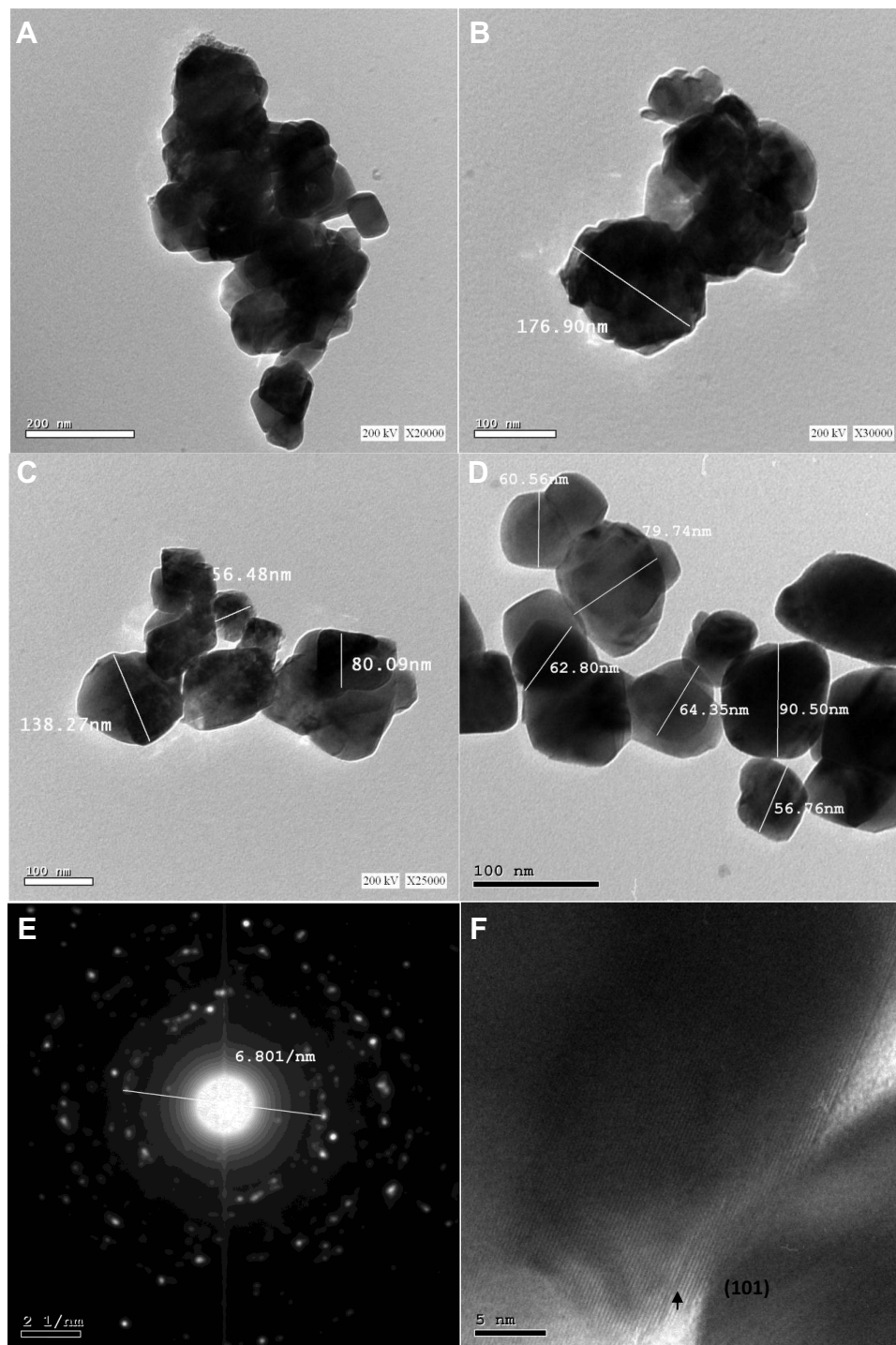
Figure 2 Shows HR-TEM images of recycled zirconia in different phases. (**A**) was pure ZrO_2 after the first, second, and third milling processes (**B**–**D**, respectively). The selected area electron diffraction pattern SEADP of ZrO_2NPs was displayed in (**E**). (**F**) presents the d-spacing, also known as lattice spacing or interplanar distance, of a crystal.

respectively. The results of the mapping images show a high spatial distribution of oxygen in the nanocomposite matrix (Figure 3D).

Zeta Potential Analysis

Using the dynamic light scattering method, the zeta potential analysis was carried out to gather information about the surface charge of the nanoparticles. The value of zeta potential can reveal the stability of the nanoparticles in the long
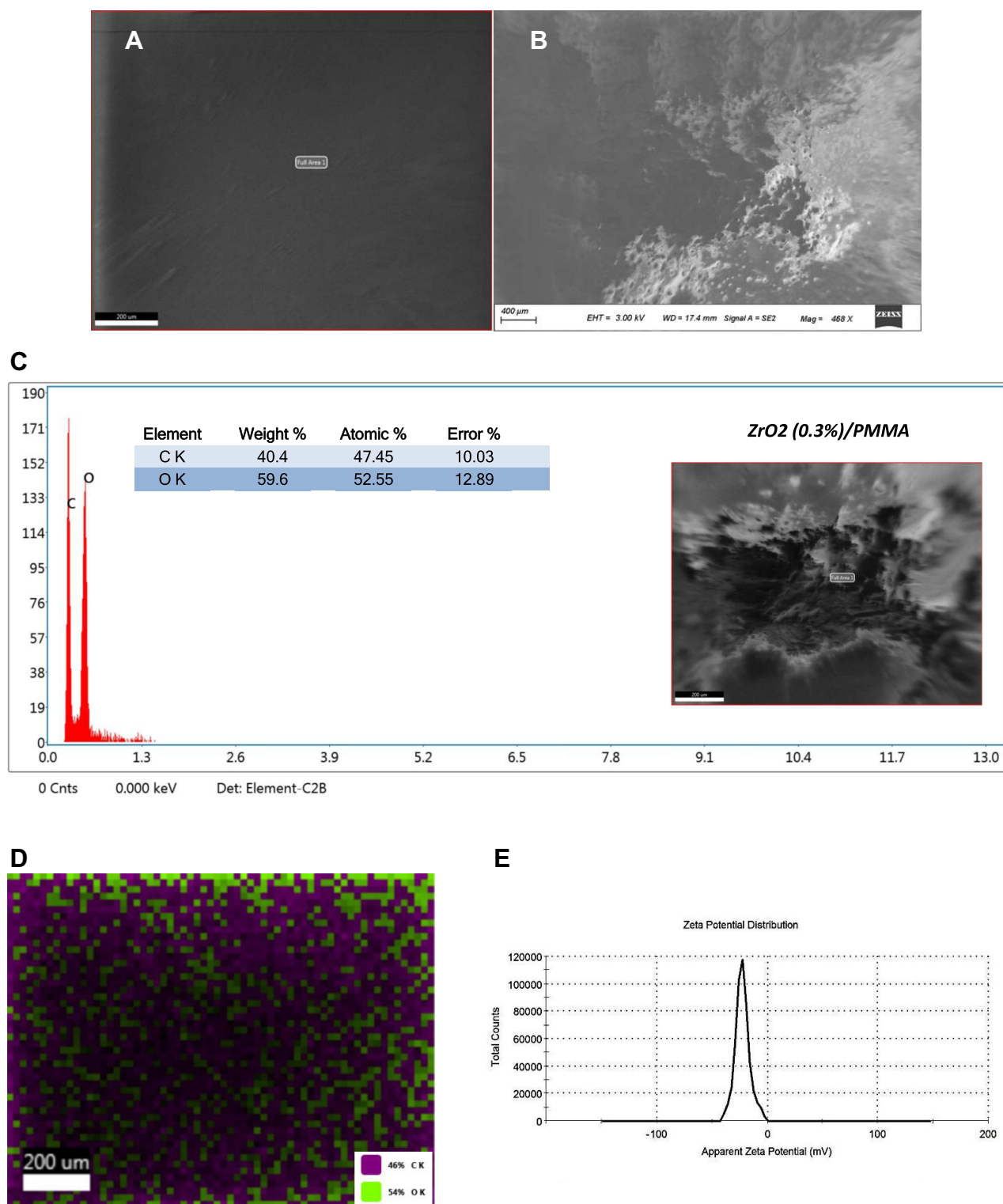
Figure 3 Shows the FESEM images of PMMA plank (**A**) and ZrO$_2$ (0.3%)/PMMA nanocomposite (**B**). (**C**) presents the EDX spectra of the ZrO2 (0.3%)/PMMA nanocomposite. (**D**), mapping images show a high spatial distribution of oxygen in the nanocomposite matrix, (**E**), represents the zeta potential spectrum.

term. A zeta value of about ±30 mV is needed for a physical suspension stabilized by the repulsion of the electrostatic role. When combining electrostatic and steric stabilization, a voltage of ±20 mV is sufficient.[30] The prepared ZrO$_2$ (0.3%)/PMMA has a zeta potential of-22.5 mV (Figure 3E). Based on the sufficient value for the stability of the solution,

the ZrO_2 (0.3%)/PMMA nanoparticles showed acceptable stability. The Zeta potential of the prepared ZrO_2 (0.3%)/PMMA is (−22.5 mV), showing acceptable stability.

Mechanical Properties

The Table 1 summarized all of the mechanical properties data, water sorption, and solubility

Impact Strength (KJ/m^2)

Figure 4 revealed a statistically significant difference between the mean impact strength of the five groups (P-value <0.001, Effect size = 0.381). Pairwise comparisons between the groups using Tukey's test revealed that the pure group (without ZrO_2) recorded the highest impact strength, with a non-statistically significant difference from the ZrO_2 0.01% group but statistically significant higher impact strength than the other groups. The group ZrO_2 0.01% showed a lower mean impact strength with a non-statistically significant difference than the pure group and the ZrO_2 0.3% group. The lowest impact strength was recorded with the ZrO_2 0.5% group, with a non-statistically significant difference from the ZrO_2 0.3% and ZrO_2 0.1% groups, but a statistically significant lower mean value compared with the pure without ZrO_2 and ZrO_2 0.01% groups. When the pure group was compared to the other groups, the ZrO_2 0.1%, ZrO_2 0.3%, and ZrO_2 0.5% groups had statistically significantly lower mean impact strength than the pure group. The ZrO_2 0.01% differed from the pure group in a non-statistically significant way, but with a lower mean impact strength.

Flexural Strength (MPa)

Again, Figure 4 displayed a statistically significant difference in the mean flexural strength of the five groups (*P*-value <0.001, Effect size = 0.396). Pairwise comparisons between the groups using Tukey's test revealed that the ZrO_2 0.3% group recorded the highest flexural strength, with a non-statistically significant difference from the ZrO_2 0.5% group and a statistically significant difference from the other groups. The lowest flexural strength was recorded with the pure group, with a non-statistically significant difference between the ZrO2 0.01% and ZrO_2 0.1% groups. When the pure group was compared to the other groups, both the ZrO_2 0.3% and ZrO_2 0.5% groups had statistically significantly higher mean flexural strength than the pure group. The ZrO_2 0.01% and ZrO_2 0.01% groups showed higher mean flexural strength than the Pure group, but it was a non-statistically significant difference.

Young's Modulus of Bending (MPa)

Also, the same Figure 4 presented a statistically significant difference between the mean Young's modulus of bending in the five groups (P-value <0.001, Effect size = 0.495). Pairwise comparisons between the groups using Tukey's test revealed that the ZrO_2 0.5% group recorded the highest Young's modulus of bending, with a non-statistically significant difference from the ZrO_2 0.3% group. There was no statistically significant difference between the ZrO_2 0.01% and ZrO2 0.1% groups; both showed statistically significantly lower mean Young's modulus of bending values. The lowest Young's modulus of bending was recorded with the pure group, with a statistically significant difference from all other groups. As regards the pair-wise comparison between the pure group and other groups, all groups containing zircon with different concentrations showed a statistically significantly higher mean Young's modulus of bending than the pure group.

Micro-Hardness (VHN)

There was a statistically significant difference in the mean micro-hardness of the five groups (P-value = 0.002, Effect size = 0.262). Pairwise comparisons between the groups using Tukey's test revealed that the ZrO_2 0.01% group recorded the highest microhardness with a statistically significant difference from all other groups. As shown in Figure 5A, there was no statistically significant difference between the pure group, the ZrO_2 0.1%), the ZrO_2 0.3%, and the ZrO_2 0.5% groups; all had statistically significant lower mean micro-hardness than the ZrO_2 0.01%.

Water Sorption (μg/mm^3)

In the Figure 5B, there was a statistically significant difference in the mean water sorption of the five groups (*P*-value <0.001, Effect size = 0.373). Pairwise comparisons between the groups using Tukey's test revealed that the ZrO_2 0.5%
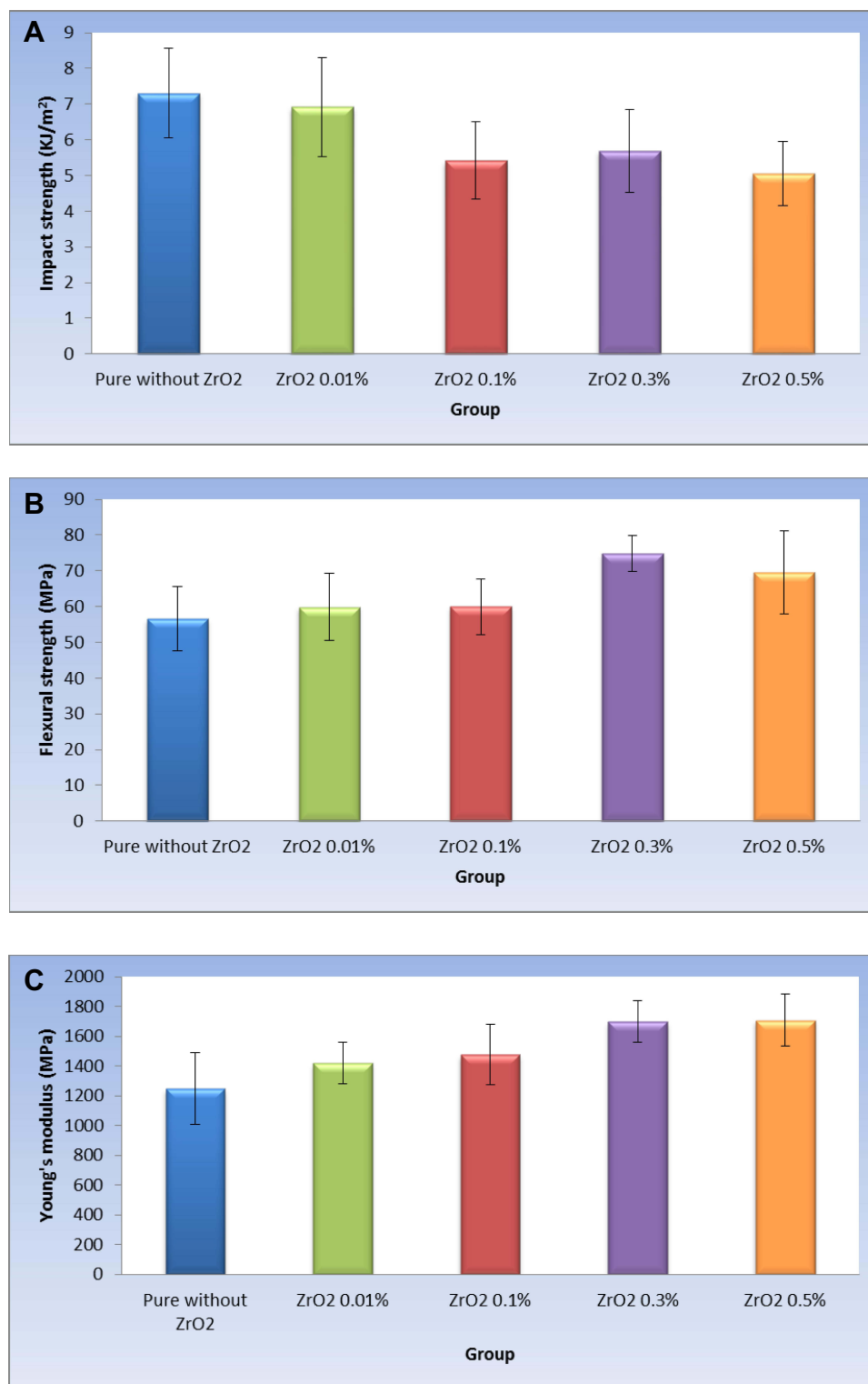
Figure 4 (**A–C**), bar chart representing mean and standard deviation values of the investigated five groups for impact strength, flexural strength, and Young's modulus of bending.

group recorded the highest water sorption with a statistically significant difference from all other groups. There was no statistically significant difference between the groups pure without ZrO_2, ZrO_2 0.01%, ZrO_2 0.1%, and ZrO_2 0.3%, all of which showed statistically significantly lower mean water sorption than the ZrO_2 0.5% group.
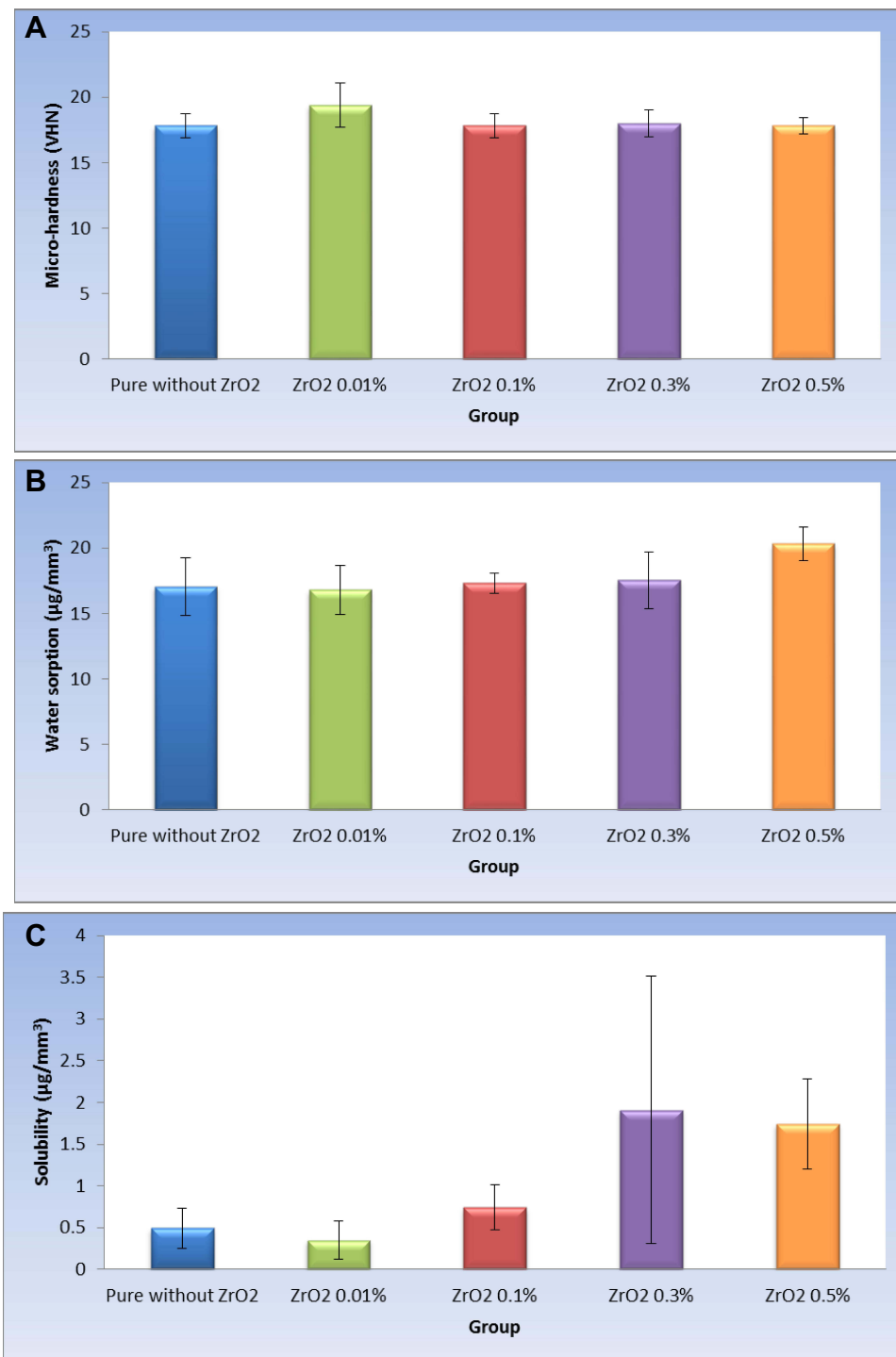
Figure 5 (A–C), bar chart representing mean and standard deviation values of the investigated five groups for micro-hardness, water sorption, and solubility.

Solubility (µg/mm3)

In the Figure 5C, there was a statistically significant difference in the mean solubility of the five groups (P-value <0.001, Effect size = 0.628). Pairwise comparisons between the groups using Dunn's test revealed that the ZrO_2 0.3% group recorded the highest solubility, with a non-statistically significant difference from the ZrO_2 0.5% group and a statistically significant difference from the other groups. There was no statistically significant difference between the pure, ZrO2 0.01%, and ZrO2 0.1% groups, all of which had statistically significantly lower mean solubility than the ZrO2 0.3% and ZrO2 0.5% groups.

Viability % Study

The Table 2 summarized all of the viability percentage data.

Comparison Between Groups

Viewing Figure 6A, after 24 hours, there was no statistically significant difference between the viability percentage values in the different groups (P-value = 0.637, effect size = 0.044). At 48 hours, there was a statistically significant difference between the viability percent values in the different groups (P-value = 0.001, effect size = 0.28). The comparisons between the groups revealed no statistically significant difference between the ZrO_2 0.01%, 0.1%, 0.3%, and ZrO_2 0.5% groups; both showed statistically significantly higher mean viability than the pure group.

Changes by Time Within Each Group

In the Figure 6B, as regards the pure group, there was a statistically significant decrease in mean viability percent after 48 hours (P-value = 0.010, Effect size = 0.185). While there was no statistically significant difference in mean viability after 48 hours for the ZrO2 0.01% (P-value = 0.634; effect size = 0.004), ZrO2 0.1% (P-value = 0.659; effect size = 0.004), ZrO2 0.3% (P-value = 0.685; effect size = 0.004), and ZrO2 0.5% (P-value = 0.801; effect size = 0.002) groups.

Discussion

With the obtained results and the statistical analysis's significant and non-significant patterns, the proposed hypothesis was accepted with limitations and should be modified. Remember, low impact, flexural, fatigue, fracture toughness, and hardness are factors that cause acrylic resin denture bases to fracture. Improving the mechanical properties and strengthening the PMMA matrix are essential for performing well. Three ways to improve the mechanical properties of PMMA are: replacing PMMA with an alternative material; chemical change; or reinforcing with other materials.[31] Researchers found that doping PMMA with an appropriate addition improved PMMA characteristics. The used additives were whiskers, rods, fibres, rubber, clay, nanoparticles, metal oxides, and wires.[32] In reviewing the literature, no data was found on the association between PMMA and recycled zirconia NPs, and this is the first study to address this point. In this context, the goal of our research was to determine the mechanical and physicochemical properties of a PMMA-based cold-cure acrylic resin combined with recycled Zirconia (ZrO_2) nano-fillers.

Indeed, the types of filler, shape, size, proportion, and distribution of the filler all have an impact on the mechanical and physical properties of the denture base.[33] It is worth mentioning that ZrO_2 was used because it has excellent

Table 2 Summarized All Data of the Viability Percentage

	Group	No. of Samples	Mean	SD	P-value	Effect Size (Eta Squared)
Viability At 24h	Pure without ZrO_2	12	97.75	3.63	0.010*	0.185
	ZrO_2 0.01%	12	98.04	4.49	0.634	0.004
	ZrO_2 0.1%	12	98.1	5.38	0.659	0.004
	ZrO_2 0.3%	12	96.56	5.51	0.685	0.005
	ZrO_2 0.5%	12	94.47	11.36	0.801	0.002
Viability (at 48h)	Pure without ZrO_2	12	89.58[B]	7.52	0.010*	0.185
	ZrO_2 0.01%	12	96.89[A]	6.06	0.634	0.004
	ZrO_2 0.1%	12	99.17[A]	1.12	0.659	0.004
	ZrO_2 0.3%	12	97.78[A]	4.01	0.685	0.005
	ZrO_2 0.5%	12	95.23[A]	6.7	0.801	0.002

Note: *Significant at $P \leq 0.05$. According to a pair-wise statistical test for comparisons among the investigated groups, the superscripts A and B indicate that these groups are statistically significant.
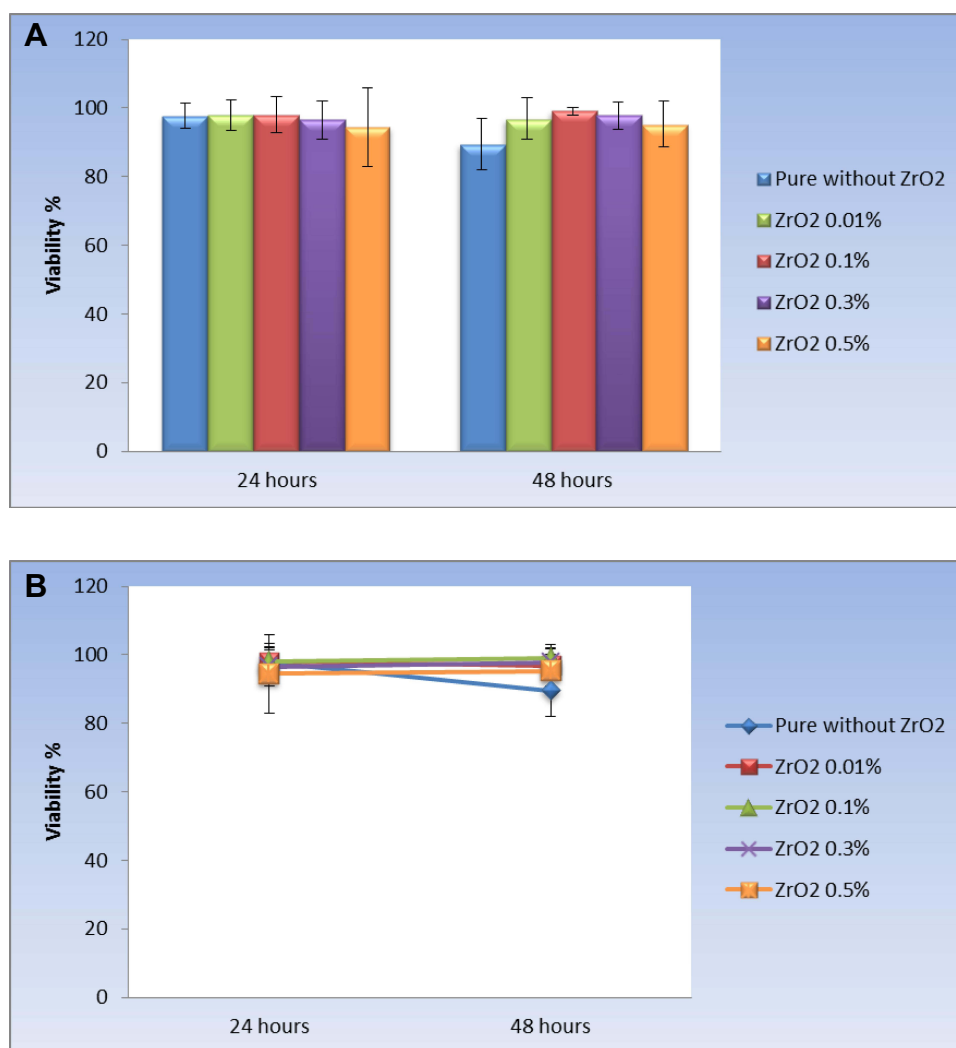
Figure 6 (**A**) bar chart representing mean and standard deviation values for viability % in the different groups, while (**B**): Line chart representing mean and standard deviation values for viability % at different time periods.

biocompatibility and a white color, which is less likely to alter aesthetics. Moreover, high fracture resistance can be acquired by ZrO_2 because of its energy retention property throughout the conversion of polygonally shaped molecules into monoclinic ones. In the current research, we used recycled Zirconia nano-filler to yield a better dispersion and eliminate aggregation by using a certain coupling agent.

Considering coupling agents, various agents, including-methacryloxypropyl-trimethoxy-Silane, 2-acetoacetoxyethyl methacrylate (AAEM), and 3-(methacryloxy) propyl-trimethoxysilane (MPTS), were used in-situ polymerization to prepare ZrO_2/PMMA.[34] The coupling agent value is to control the interface properties and improve the mechanical properties and optical properties of ZrO_2/PMMA nanocomposites because of its ability to attach the ZrO_2 on one side while favouring the dispersion on the other.[35] In this research, we chose a hydroxyl group-containing agent, HEMA, to aid in the dispersion of the recycled ZrO_2 NPs in MMA. Because the HEMA molecule is bi-functional (hydroxyl and vinyl groups), it operates as a bridge between the PMMA matrix and ZrO_2 NPs, preventing phase separation caused by depletion force during in situ polymerization. The HEMA agent is attached to the surface of ZrO_2 NPs via hydrogen bonding. Also, the hydrogen bonding interaction between the polymer matrix and ZrO_2 NPs would possibly occur in ZrO_2/PMMA nanocomposites.

Again, in this study, formulae comprising different percentages (0.01%, 0.1%, 0.3%, and 0.5%) of recycled ZrO_2 NPs-HEMA to mono-methyl methacrylate (MMA monomer) were prepared and mixed with PMMA (polymer) powder

to get the chemical bond between ZrO_2 NPs and PMMA. The dispersion of ZrO_2 NPs in MMA without agglomeration was achieved via the HEMA ligand. We ensured the dispersion by measuring the zeta potential. It was about-22.5 mV, as mentioned. The optimal procedure for preparing HEMA functionalized ZrO_2 NPs in MAA to achieve good dispersion was: the HEMA-to-ZrO_2 molar ratio was 0.8:1, the ZrO_2 concentration was low wt% (0.01, 0.1, 0.3, and 0.5), the sonication duration was 20 minutes at room temperature, the heating period was 20 hours at 60 degrees Celsius, and there was no stirring.

Regarding the formula ZrO_2 NPS-HEMA-MMA-PMMA, it has a good chance of chemical bonding. The reason for this exists in the atomic number of zirconium, Zr of 40, containing unsaturated empty orbitals (5S and 4d), which can be attacked by the single pair electron of each (O) present in the HEMA agent and PMMA polymer to create coordination bonds with ZrO_2 NPs fillers.[36] Furthermore, covalent bonding and physical molecular interaction by Vander Waal forces can occur at the PMMA-ZrO_2 NPs interface to increase adhesion force, which is a factor affecting the mechanical properties of the resin.[37] Importantly, we considered three factors. The first was the amount and percentage of the recycled ZrO_2 NPs fillers, where the increase in the filler fraction does not necessarily lead to an increase in the strength, because excessive filler fractions can create more cracks and defects. The second was the ZrO_2 filling that should be interstitial, and the filler ZrO_2NPs should disperse evenly into the PMMA matrix without interrupting the continuity of the matrix. The third is the cytotoxicity of the recycled ZrO_2 NPs. It was reported that high percentages above 7% lead to massive changes in the colour of acrylic.[38] As mentioned, we preferred to select low percentage values for this issue.

Again, in this study, the mentioned mechanical tests were performed to prove whether the recycled zirconia is a potential reinforcement for the acrylic denture base polymer. Impact strength is one of the most important mechanical properties of acrylic resin. The impact test measures the energy required to break the specimen by applying a dynamic load.[39] The total measured energy includes kinetic, frictional, and vibrational energies that are not correlated with the fracture resistance of the denture base material. The test methodology depends on specimen dimensions, notch depth, radius, impact velocity, etc.[40]

The results showed substantial changes in impact strength between the means, demonstrating that the percent of recycled ZrO_2 NPs influenced impact strength. However, an increase in ZrO_2 does not mean an increase in impact strength. Figure 4 reveals that the modified ZrO_2 NPs at 0.5wt% lead to a reduction in impact strength. Excessive filler fractions may cause additional defects, making the material more vulnerable to damage. Many suggested explanations, including the higher surface area of the fillers and stress concentration, lead to the crack proportion. Also, the increase in the percentage of modified-nano-ZrO_2 powder affects the interface region, leading to a lowering of energy dissipation per unit volume and consequently lowering the impact strength.[41] A good explanation of the effect of higher filler content on reducing strength can be explained on the basis that, after reaching a saturation point, the resin cannot incorporate any further filler particles. Any attempt to add filler particles after reaching saturation of the matrix leads to an interruption in the resin matrix continuity, thus causing a decrease in the strength of reinforced specimens. The results obtained are consistent with previous studies.[42]

Flexural strength is a material parameter. It is also known as the modulus of rupture, bend strength, or transverse rupture strength. The flexural strength test is a requisite mechanical test for denture base polymers as recommended by ADA specification No. 12 and ISO 1220795-1. Because it simulates the exerted stress on the denture during mastication, the flexural three-point bending test is convenient for studying denture base materials.

We investigated the flexural strength of denture base resin since it is the most common cause of clinical failure. The flexural strength results are listed in Table 1 and are depicted in Figure 4, which shows that the denture base flexural strength increased with ZrO_2 incorporation at loading (0.01, 0.1, and 0.3wt%) but decreased with constant ZrO_2 addition (0.5 wt%). To explain this, at 0.01, 0.1, and 0.3wt%, the HEMA coupling agent eliminated ZrO_2 aggregation, achieved the well-dispersion of ZrO_2 NPs, and allowed them to enter between the PMMA's linear macromolecular chains and fill the spaces between the chains, resulting in increased resin strength and rigidity, which improves fracture resistance and leads to enhanced flexural strength, gradually. While the flexural strength started to decrease at 0.5 wt%, this may be due to irregular ZrO_2 distribution in the PMMA. Another reason is the decrease in the bonding filler particles and the PMMA matrix. Also, the excess fillers could separate PMMA chains and exert weak forces between them, leading to a decrease in the polymer's fracture resistance and mechanical properties.

4654

International Journal of Nanomedicine 2022:17

Overall, the outcome of the current investigation showed a very clear and significant difference in the mean flexural strength among the recycled zirconia percent. The residual monomer was the source of this difference. Because of the plasticizing effect of the residual monomer, which minimizes interchange forces, it may affect flexural strength.[43] The strength, number, and nature of the bonds between the recycled zirconia nanoparticles and the PMMA matrix also play a role in the difference. Ban Saad Jasim et al came to similar conclusions.[44] Yingying Pan reported similar findings, stating that the flexural strength increased initially after the inclusion of hydroxyapatite HAP with PMMA, but thereafter decreased with continual HAP addition.[45] However, Wei Yu reported that, unlike ZrO_2 nanoparticles, the flexural strength of the surface-treated ZrO_2 nanotube/PMMA composite was lower than that of its untreated counterpart in this context.[46]

Another mechanical test was Young's modulus, which is often known as the modulus of elasticity. It measures the material's ability to endure length changes when under lengthwise tension or compression. Figure 4 revealed a direct correlation between the modulus of elasticity and the incorporated percent of the recycled ZrO_2 NPs. However, it was non-significant. We attributed the mean difference and the ZrO_2% to the strength and number of primary bonds.

Hardness is the material's resistance to deformation when measured under an indentation load. The hardness test evaluates the degree of conversion during the resin polymerization reaction between powder spheres of polymethyl methacrylate and methyl methacrylate with hydroquinone as a liquid and a small amount of benzoyl peroxide as a chemical activator. The degree of conversion of composite materials indicates the distribution and quantity of inorganic fillers. The two hardness tests are macro hardness and microhardness. Macro hardness relates to testing with a load of over a kilogram, or around 10 Newton (N). Microhardness testing is convenient for smaller samples, thin specimens, plated surfaces, or thin films that have an applied stress of less than 10 N.[47] A substance's micro-hardness is measured using an indenter that penetrates microscopic areas.[48]

In this study, we applied micro Vickers hardness VH, which reflects the uniformity of reinforcement dispersion in composites, evaluates conversion degree during the resin polymerization reaction, and the effect of crosslinking density on micro-level. Table 2 represents VH values for PMMA matrix and non-aqueous-recycled ZrO_2/PMMA nanocomposites. Figure 4 reveals no significant difference between the pure group, 0.1%, 0.3% and 0.5% groups, but all showed a significantly lower mean micro-hardness than the ZrO_2 0.01%.

Deterioration of the polymeric matrix reduces acrylic hardness, increases the chance of cracking, and shortens the denture base's longevity. Improvements in VH using recycled ZrO_2 nano fillers are related to the ZrO_2 particles' intrinsic properties. Strong ionic interatomic bonding characterises ZrO_2, resulting in its desirable material properties of hardness and strength. However, the low VH values presented by 0.1, 0.3, and 0.5% might be because of an incomplete monomer conversion affected by the increase in filler content, suggesting a high residual monomer after the polymerization process. The residual monomer acts as a plasticizer, reducing the material resistance. The highest VH value for 0.01% zirconia suggests a small amount of residual monomer content and therefore a high monomer conversion during the polymerization process. We disagreed with Ruaa et al, who claimed hardness increases by increasing the ZrO2 particle size.[49]

Water sorption and solubility are essential issues that determine denatured base durability. The PMMA polarity and the diffusion of water molecules into the interstitial spaces between polymer chains influence water absorption.[50] Water acts as a plasticizer, interacts with the polymer chains, and changes the mechanical properties, color, and dimensional stability. In the current study, we used the method that is recommended by ISO for measuring water sorption and solubility. Water sorption was determined according to an increase in mass per unit volume and solubility according to the loss of mass from polymers.

Table 1 shows the values for water sorption. The values lie within the ADA Specification No. 12 that recommends water sorption should not exceed 0.8 mg/cm³. The 0.5% displayed the highest sorption. The increase in the water sorption differs according to the percent of the recycled ZrO_2 NPs compared to the control group specimens. We attributed water sorption to weak secondary bonds in PMMA. Further, the addition of the recycled ZrO_2 NPs into the monomer increased the polarity and permeability of the PMMA. Increasing the PMMA permeability allowed water to reach the interface between PMMA and ZrO_2 NPs. This interface is water sensitive because of the high surface energy of the ZrO_2 NPs. Thus, increased filler concentration leads to an increased particle–polymer interface, which leads to increased water sorption. The current study agreed with Zuccari et al,[51] who concluded that the zirconia

particles increase water sorption by the resin systems. However, this decreased the impact strength, as shown in Figure 5.

Regarding solubility, 0.3% showed the highest water solubility value. It may indicate leaching out of the monomer over time and a lesser conversion of the monomer to polymerized polymer chains. It is important to determine the residual monomer content and solubility of the tested materials, as these properties influence the allergy susceptibility of these materials. For this reason, this study evaluated the water sorption and solubility of different percentages of recycled ZrO_2 NPs in acrylic resins. However, more research is needed to see how recycled ZrO_2 NPs reinforcement affects denture base resins when specimens are held in water or artificial saliva for long periods.

Schmalz and Browne stated that for biocompatibility of dental materials, appropriate host responses are necessary.[52] In dentistry, this means no adverse reaction or a tolerable adverse reaction of the living system to the material. In this context, one of the aims of this study was to evaluate the cytotoxicity of the prepared acrylic resin in vitro using an MTT test that has been frequently used for evaluating acrylic resin. The cytotoxic effect of the specimens was determined versus WI38 normal lung cells. When the cells were incubated with the resins for 24 hours, Figure 6 displays no statistically significant difference between the viability percentage values in the different groups. However, one can see that there was a slightly cytotoxic effect of 0.5%. The most surprising aspect of the data is when the incubation lasted for 48 hours, the viability percent of the investigated percentages was higher than the pure one, as shown in the same figure.

Conclusion

Polymethyl methacrylate's mechanical strength is still incompetent to protect denture longevity, and novel nanostrategies are emerging to address dental issues. In this study, recycled ZrO2 NPs were obtained as a by-product of milling procedures, and formulae including 0.01%, 0.1%, 0.3%, and 0.5% recycled ZrO2NPs-HEMA were synthesized and mixed with PMMA polymer powder in various proportions. According to our findings, PMMA with those ratios of recycled ZrO2 nanofillers has the potential to be a reliable denture base material with improved flexural strength, modulus of elasticity, and hardness. The optimal concentration was 0.3% wt. ZrO_2. Our findings show that the longer the resin is allowed to elute, the less cytotoxic it is.

Data Sharing Statement

The authors emphasize the availability of data and materials.

Ethics Approval and Consent to Participate

The authors followed the ethics of research, approved and consented to participate in this study.

Consent for Publication

The authors consent this manuscript for publication.

Disclosure

The authors report no competing interests in this work.

References

1. Zafar MS. Prosthodontic applications of polymethyl methacrylate (PMMA): an update. *Polymers*. 2020;12(10):1–35. doi:10.3390/polym12102299
2. Samad HA, Jaafar M. Effect of polymethyl methacrylate (PMMA) powder to liquid monomer (P/L) ratio and powder molecular weight on the properties of PMMA cement. *Polym Plast Technol Eng*. 2009;48(5):554–560. doi:10.1080/03602550902824374
3. Bayraktar G, Guvener B, Bural C, Uresin Y. Influence of polymerization method, curing process, and length of time of storage in water on the residual methyl methacrylate content in dental acrylic resins. *J Biomed Mater Res*. 2006;76(2):340–345. doi:10.1002/jbm.b.30377
4. Faltermeier A, Rosentritt M, Müssig D. Acrylic removable appliances: comparative evaluation of different postpolymerization methods. *Am J Orthod Dentofac Orthop*. 2007;131(3):301.e16–301.e22. doi:10.1016/j.ajodo.2006.07.019
5. Bernardi MIB, Rojas SS, Andreeta MRB, De Rastelli NS, Hernandes C, Bagnato VS. Thermal analysis and structural investigation of different dental composite resins. *J Therm Anal Calorim*. 2008;94(3):791–796. doi:10.1007/s10973-008-8820-x
6. May LW, Seong LG. A narrative review of different types and processing methods of acrylic denture base material. *Ann Dent*. 2018;25(2):58–67. doi:10.22452/adum.vol25no2.7
7. McCracken WL. Auxiliary uses of cold-curing acrylic resins in prosthetic dentistry. *J Am Dent Assoc*. 1953;47(3):298–304. doi:10.14219/jada.archive.1953.0166
8. Kawara M, Komiyama O, Kimoto S, Kobayashi N, Kobayashi K, Nemoto K. Distortion behavior of heat-activated acrylic denture-base resin in conventional and long, low-temperature processing methods. *J Dent Res*. 1998;77(6):1446–1453. doi:10.1177/00220345980770060901
9. Elvira C, Levenfeld B, Vázquez B, San Román J. Amine activators for the 'cool' peroxide initiated polymerization of acrylic monomers. *J Polym Sci Part A Polym Chem*. 1996;34(13):2783–2789. doi:10.1002/(SICI)1099-0518(19960930)34:13<2783::AID-POLA24>3.0.CO;2-7
10. Khalil BI, Gharkan KS, Aliwi H. Study of Some mechanical and physical properties of cold curing Acrylic resin reinforced with particle yttrium oxide. *J Coll Basic Educ Pure Sci*. 2016;23(97):1–12.
11. So YC, Tsoi JKH, Matinlinna JP. A new approach to cure and reinforce cold-cured acrylics. *Silicon*. 2012;4(3):209–220. doi:10.1007/s12633-012-9124-0
12. Hamedi-Rad F, Ghaffari T, Rezaii F, Ramazani A. Effect of nanosilver on thermal and mechanical properties of acrylic base complete dentures. *J Dent*. 2014;11(5):495–505.
13. Priyadarsini S, Mukherjee S, Mishra M. Nanoparticles used in dentistry: a review. *J Oral Biol Craniofacial Res*. 2018;8(1):58–67. doi:10.1016/j.jobcr.2017.12.004
14. Ash BJ, Rogers DF, Wiegand CJ, et al. Mechanical properties of Al2O3/polymethylmethacrylate nanocomposites. *Polym Compos*. 2002;23(6):1014–1025. doi:10.1002/pc.10497
15. Al-Kawaz A, Rubin A, Badi N. Tribological and mechanical investigation of acrylic-based nanocomposite coatings reinforced with PMMA-grafted-MWCNT. *Mater Chem Phys*. 2016;175:206–214. doi:10.1016/j.matchemphys.2016.03.021
16. Singh SK, Singh S, Kumar A, Jain A. Thermo-mechanical behavior of TiO2 dispersed epoxy composites. *Eng Fract Mech*. 2017;184:241–248. doi:10.1016/j.engfracmech.2017.09.005
17. Navidfar A, Azdast T, Ghavidel AK. Influence of processing condition and carbon nanotube on mechanical properties of injection molded multi-walled carbon nanotube/poly methyl methacrylate nanocomposites Influence of processing condition and carbon nanotube on mechanical properties of inj. *J Appl Polymer Sci*. 2016. doi:10.1002/app.43738
18. Alamgir M, Mallick A, Nayak GC, Tiwari SK. Development of PMMA/TiO2 nanocomposites as excellent dental materials. *J Mech Sci Technol*. 2019;33(10):4755–4760. doi:10.1007/s12206-019-0916-7
19. Chevalier J, Gremillard L, Virkar AV, Clarke DR. The tetragonal-monoclinic transformation in zirconia: lessons learned and future trends. *J Am Ceram Soc*. 2009;92(9):1901–1920. doi:10.1111/j.1551-2916.2009.03278.x
20. Vojdani M, Bagheri R, Khaledi AAR. Effects of aluminum oxide addition on the flexural strength, surface hardness, and roughness of heat-polymerized acrylic resin. *J Dent Sci*. 2012;7(3):238–244. doi:10.1016/j.jds.2012.05.008
21. Hu Y, Gu G, Zhou S, Wu L. Preparation and properties of transparent PMMA/ZrO2 nanocomposites using 2-hydroxyethyl methacrylate as a coupling agent. *Polymer*. 2011;52(1):122–129. doi:10.1016/j.polymer.2010.11.020
22. Ibrahim A. A modified flasking technique for complete denture base processing with sandy acrylic resin. *Int J Appl Dent Sci*. 2016;2(4):1–3.
23. American Society for Testing and Materials. Standard test method for determining the charpy impact resistance of notched specimens of plastics. *ASTM*. 2010;17. doi:10.1520/D6110-10.1
24. Jin J, Takahashi H, Iwasaki N. Effect of test method on flexural strength of recent dental ceramics. *Dent Mater J*. 2004;23(4):490–496. doi:10.4012/dmj.23.490
25. Novitskaya E, Chen P-Y, Hamed E, et al. Recent advances on the measurement and calculation of the elastic moduli of cortical and trabecular bone: a review. *Theor Appl Mech*. 2011;38(3):209–297. doi:10.2298/tam1103209n
26. Agarwal B, Patel C, Singh BP, Kumar A, Singh M, Singh N. Water sorption and solubility of denture base resins- an evaluation. *Indian J Appl Res*. 2015;5(8):41–44.
27. Berridge MV, Herst PM, Tan AS. Tetrazolium dyes as tools in cell biology: new insights into their cellular reduction. *Biotechnol Annu Rev*. 2005;11:127–152. doi:10.1016/S1387-2656(05)11004-7
28. Garnweitner G, Goldenberg LM, Sakhno OV, Antonietti M, Niederberger M, Stumpe J. Large-scale synthesis of organophilic zirconia nanoparticles and their application in organic-inorganic nanocomposites for efficient volume holography. *Small*. 2007;3(9):1626–1632. doi:10.1002/smll.200700075
29. Reyes-Acosta M, Torres-Huerta M, Domínguez-Crespo M, Flores-Vela I, Dorantes-Rosales HJ, Ramírez-Meneses E. Influence of ZrO2 nanoparticles and thermal treatment on the properties of PMMA/ZrO2 hybrid coatings. *J Alloys Compd*. 2015;643(S1):S150–S158. doi:10.1016/j.jallcom.2014.10.040
30. Izadiyan Z, Shameli K, Miyake M, et al. Cytotoxicity assay of plant-mediated synthesized iron oxide nanoparticles using Juglans regia green husk extract. *Arab J Chem*. 2020;13(1):2011–2023. doi:10.1016/j.arabjc.2018.02.019
31. Kim SH, Watts DC. The effect of reinforcement with woven E-glass fibers on the impact strength of complete dentures fabricated with high-impact acrylic resin. *J Prosthet Dent*. 2004;91(3):274–280. doi:10.1016/j.prosdent.2003.12.023

32. Salahuddin N, El-Kemary M, Ibrahim E. Reinforcement of polymethyl methacrylate denture base resin with ZnO nanostructures. *Int J Appl Ceram Technol*. 2018;15(2):448–459. doi:10.1111/ijac.12802

33. Gad MM, Abualsaud R, Rahoma A, Al-Thobity AM, Al-Abidi KS, Akhtar S. Effect of zirconium oxide nanoparticles addition on the optical and tensile properties of polymethyl methacrylate denture base material. *Int J Nanomedicine*. 2018;13:283–292. doi:10.2147/IJN.S152571

34. Otsuka T, Chujo Y. Poly(methyl methacrylate) (PMMA)-based hybrid materials with reactive zirconium oxide nanocrystals. *Polym J*. 2010;42 (1):58–65. doi:10.1038/pj.2009.309

35. Collares FM, Ogliari FA, Zanchi CH, Petzhold CL, Piva E, Samuel SMW. Influence of 2-hydroxyethyl methacrylate concentration on polymer network of adhesive resin. *J Adhes Dent*. 2011;13(2):125–129. doi:10.3290/j.jad.a18781

36. Hameed HK, Rahman HA. The effect of addition nano particle ZrO2 on some properties of autoclave processed heat cure acrylic denture base material. *J Baghdad Coll Dent*. 2015;27(1):32–39. doi:10.12816/0015262

37. Sun L, Gibson RF, Gordaninejad F, Suhr J. Energy absorption capability of nanocomposites: a review. *Compos Sci Technol*. 2009;69 (14):2392–2409. doi:10.1016/j.compscitech.2009.06.020

38. Ellakwa AE, Morsy M, El-Sheikh AM. Effect of aluminum oxide addition on the flexural strength and thermal diffusivity of heat-polymerized acrylic resin. *J Prosthodont*. 2008;17(6):439–444. doi:10.1111/j.1532-849X.2008.00318.x

39. Komurlu E. An experimental study on determination of crack propagation energy of rock materials under dynamic (impact) and static loading conditions. *Hittite J Sci Eng*. 2019;6(1):01–06. doi:10.17350/hjse19030000126

40. Alhotan A, Yates J, Zidan S, Haider J, Silikas N. Assessing fracture toughness and impact strength of PMMA reinforced with nano-particles and fibre as advanced denture base materials. *Materials*. 2021;14(15):4127. doi:10.3390/ma14154127

41. Maheshwari R, Abrol K, Agarwal SK, Singhal R, Agarwal S. Evaluation of impact strength and surface hardness of acrylic resin modified with different nano materials: an in vitro study. *Int J Prosthodont Restor Dent*. 2019;9(4):113–116. doi:10.5005/jp-journals-10019-1254

42. Ashour Ahmed M, El-Shennawy M, Althomali YM, Omar A. Effect of titanium dioxide nano particles incorporation on mechanical and physical properties on two different types of acrylic resin denture base. *World J Nano Sci Eng*. 2016;06(03):111–119. doi:10.4236/wjnse.2016.63011

43. Singh K, Ohlan A, Saini P, Dhawan SK. composite – super paramagnetic behavior and variable range hopping 1D conduction mechanism – synthesis and characterization. *Polym Adv Technol*. 2008;19:229–236. doi:10.1002/pat.1003

44. Jasim S, Mohammed DH, Fatalla A. Effect of modified alumina nanofillers addition on thermal properties and some other properties of heat cured acrylic soft lining material. 2018.

45. Pan Y, Liu F, Xu D, Jiang X, Yu H, Zhu M. Novel acrylic resin denture base with enhanced mechanical properties by the incorporation of PMMA-modified hydroxyapatite. *Prog Nat Sci Mater Int*. 2013;23(1):89–93. doi:10.1016/j.pnsc.2013.01.016

46. Yu W, Wang X, Tang Q, Guo M, Zhao J. Reinforcement of denture base PMMA with ZrO2 nanotubes. *J Mech Behav Biomed Mater*. 2014;32:192–197. doi:10.1016/j.jmbbm.2014.01.003

47. Broitman E. Indentation hardness measurements at macro-, micro-, and nanoscale: a critical overview. *Tribol Lett*. 2017;65(1):1–18. doi:10.1007/s11249-016-0805-5

48. Yovanovich MM. Micro and macro hardness measurements, correlations, and contact models. *Collect Tech Pap*. 2006;16:11702–11729. doi:10.2514/6.2006-979

49. Chou T, Kelly A. Mechanical properties of composites. *Annu Rev Mater Sci*. 1980;10(1):229–259. doi:10.1146/annurev.ms.10.080180.001305

50. Itoh S, Nakajima M, Hosaka K, et al. Dentin bond durability and water sorption/solubility of one-step self-etch adhesives. *Dent Mater J*. 2010;29 (5):623–630. doi:10.4012/dmj.2010-028

51. Zuccari AG, Oshida Y, Moore BK, et al. Reinforcement of acrylic resins for provisional fixed restorations. Part I: mechanical properties. *Biomed Mater Eng*. 1997;7(5):327–343.

52. Schmalz G. Biological evaluation of medical devices: a review of EU regulations, with emphasis on in vitro screening for biocompatibility. *Altern Lab Anim*. 1995;23(4):469–473. doi:10.1177/026119299502300408